Aspect-dependent variations in regolith creep revealed by meteoric ¹⁰Be

Nicole West¹, Eric Kirby², Paul Bierman³, and Brian A. Clarke¹

Department of Geosciences, Pennsylvania State University, University Park, Pennsylvania 16802, USA

²College of Earth, Ocean, and Atmospheric Sciences, Oregon State University, Corvallis, Oregon 97331, USA

³Department of Geology, and Rubenstein School of Environment and Natural Resources, University of Vermont, Burlington, Vermont 05405, USA

ABSTRACT

Although variations in insolation and emergent feedbacks among soil moisture, vegetation, and soil cohesion are commonly invoked to explain topographic asymmetry that depends on aspect, few studies have directly quantified the efficiency of regolith transport along hillslopes of opposing aspect. We utilize meteoric 10 Be concentrations in regolith (n = 74) to determine mass flux along equatorial-facing and polar-facing hillslopes in three forested upland watersheds in and adjacent to the Susquehanna Shale Hills Critical Zone Observatory in central Pennsylvania (USA). In combination with regolith depth measurements and high-resolution topography, these fluxes allow us to evaluate transport rate laws and the efficiency of regolith creep. Concentrations of meteoric ¹⁰Be in regolith along six separate transects imply that regolith flux is similar along all hillslopes, despite differences in topographic gradient and regolith thickness. Comparison of flux with regolith depth and topographic gradient reveals that transport depends on regolith depth, and that regolith creep is twice as efficient along low-gradient, south-facing slopes with thin regolith as compared to steep, north-facing slopes mantled with thicker regolith. We suggest that the observed topographic asymmetry in these watersheds has evolved over geologic time as a result of differences in the frequency of freezethaw events between hillslopes of opposing aspect.

INTRODUCTION

Topographic asymmetry that depends on the facing direction, or aspect, of hillslopes is a common yet enigmatic characteristic of natural landscapes (e.g., Melton, 1960; Hack and Goodlett, 1960). Global analyses of topographic asymmetry suggest that equatorial-facing hillslopes are, on average, shallower than polarfacing hillslopes at mid-latitudes (Poulos et al., 2012), although deviations exist in some arid and glacial landscapes (e.g., Gilbert, 1904; Naylor and Gabet, 2007; Burnett et al., 2008). Aspect-dependent differences in hillslope angles present a challenge to models that consider transport efficiency to be uniform across landscapes (e.g., Perron et al., 2009) as they implicate potentially important feedbacks between microclimate and topography. In arid and semiarid landscapes, differences in insolation are thought to lead to variations in soil moisture, vegetation, runoff processes, and effective soil cohesion (e.g., Istanbulluoglu et al., 2008) that in turn influence the efficacy of regolith creep (e.g., Pierce and Colman, 1986). Recent studies suggest that asymmetry may also evolve in alpine landscapes as a consequence of thermally driven differences in frost shattering and creep efficiency (Anderson et al., 2013). However, no studies have directly measured mass transport rates or efficiency across asymmetric watersheds and, thus, our understanding of these phenomena remains largely inferential.

Hillslope gradients reflect the dynamic balance between relative base level fall and

downslope regolith flux (e.g., Culling, 1963; Kirkby, 1971). We define regolith as the layer of chemically and physically altered material formed from weathered, but intact, parent bedrock. The simplest description of downslope regolith flux asserts that transport is linearly proportional to the local hillslope gradient, which in one dimension is

$$q = K_1 \frac{dz}{dx},\tag{1}$$

where q is the volumetric regolith flux per unit width along slope (cm 2 yr $^{-1}$), K_1 is analogous to a diffusion coefficient (cm² yr⁻¹) describing the transport efficiency of creep processes, and dz/ dx is the local hillslope gradient. Equation 1 successfully describes much of the first-order structure of landscape topography; however, emerging evidence suggests that a depth-dependent transport rule may be more appropriate for disturbance-driven regolith creep (Heimsath et al., 2005; Yoo et al., 2007; Roering, 2008; Pelletier et al., 2011). Considering that the probability of disturbance-driven regolith transport decreases with depth, a transport law that considers regolith flux to depend on local hillslope gradient, regolith depth, and some characteristic mixing depth can be written as

$$q = -K_2 \left[1 - e^{-h/h^*} \left(1 + \frac{h}{h^*} \right) \right] \frac{dz}{dx}, \tag{2}$$

where K_2 is a diffusion coefficient (cm² yr⁻¹), h is the creeping regolith thickness (cm), and h^* is the characteristic mixing depth (cm) of processes driving downslope regolith creep such

as freeze-thaw and/or bioturbation (e.g., Anderson, 2002). In contrast to some depth-dependent models that consider transport to be linearly dependent on the product of regolith depth and slope (e.g., Heimsath et al., 2005; Roering, 2008), this formulation acknowledges that regolith depth and the base of a mobile layer need not be coincident.

During the past two decades, the application of meteoric ¹⁰Be to the study of Earth surface processes (e.g., Monaghan et al., 1992; McKean et al., 1993; Jungers et al., 2009; West et al., 2013) has allowed direct estimates of downslope regolith flux on eroding hillslopes, provided that the delivery rate of ¹⁰Be can be estimated (Willenbring and von Blanckenburg, 2010; Graly et al., 2011). Accounting for the mass balance of meteoric ¹⁰Be in creeping regolith, the volumetric downslope flux (*q*) of regolith (in cm² yr⁻¹) can be calculated as:

$$q_{x} = \frac{Dm_{a}}{C \rho} (x - x_{0}), \tag{3}$$

where D is the meteoric ¹⁰Be delivery rate (in atoms cm⁻² yr⁻¹), m_a is the atomic mass of ¹⁰Be, C_{re} is the concentration of ¹⁰Be in regolith (g/g sample), ρ_{re} is the depth-averaged bulk density of regolith, and $x - x_0$ is the distance between the sample location and the ridge top (Monaghan et al., 1992; McKean et al., 1993; West et al., 2013).

In this study, we use meteoric ¹⁰Be to explore the origin of asymmetric regolith-mantled hillslopes within three first-order watersheds in and adjacent to the Susquehanna Shale Hills Critical Zone Observatory (SSHO), located in central Pennsylvania (USA). During the late Pleistocene, the terminus of the Laurentide ice sheet was ~75 km due north, and the region of the SSHO had a periglacial climate (Clark and Ciolkosz, 1988). All three watersheds have a central channel oriented approximately east-west, and all exhibit steeper north-facing hillslopes than south-facing hillslopes (Fig. 1). Hillslopes are characterized by convex-up ridge tops, planar mid-slopes, and concave-up toe slopes (West et al., 2013). Bedding strikes at a high angle to the axis of the catchments ($\sim 50^{\circ}$) and dips steeply to the northwest ($\sim 50^{\circ}$), thus, the topographic asymmetry is not a direct reflection of dipping strata. Although previous studies noted this asymmetry (Ma et al., 2013; West et al., 2013), the cause of its development remains unknown.

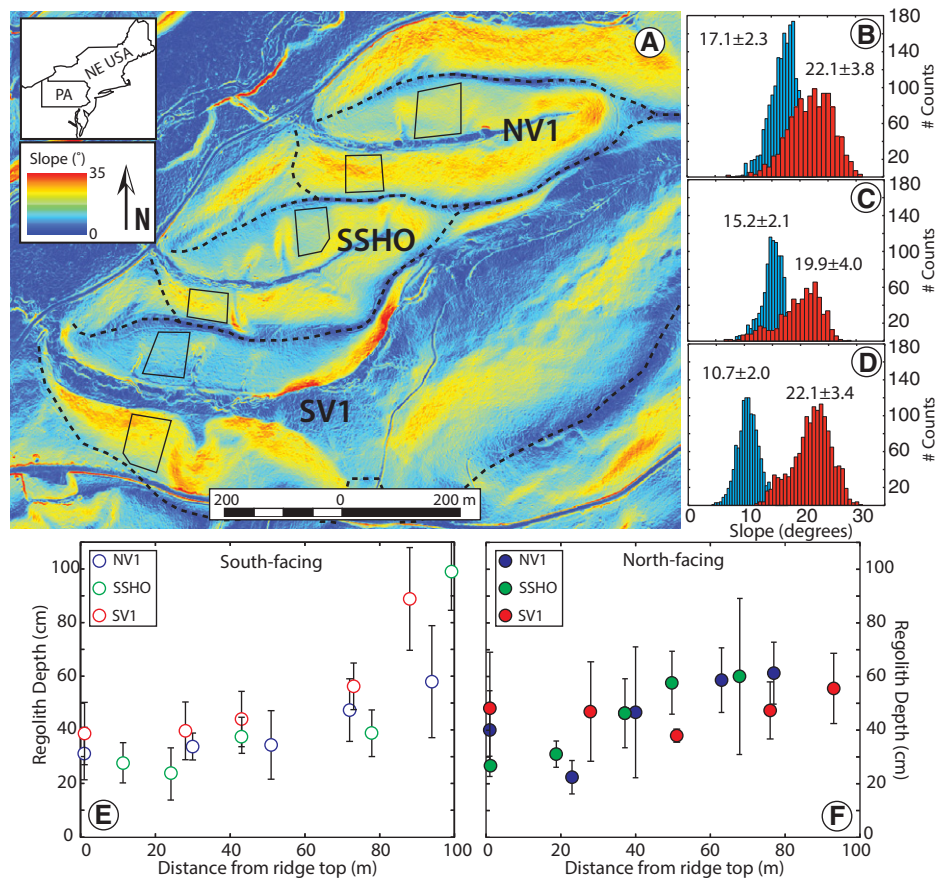


Figure 1. A: Topographic gradient of watersheds in and adjacent to Shale Hills Critical Zone Observatory (SSHO). NE—northeast; PA—Pennsylvania; NV1—north valley; SV1—south valley. B–D: Distribution of gradients from sampled regions of planar hillslopes (solid black boxes) along north-facing (orange) and south-facing (blue) hillslopes. B: NV1. C: SSHO. D: SV1. E: Depth to refusal for hand auger along south-facing hillslopes. Error bars represent one standard deviation of the mean auger depth at each position. F: Depth to refusal for hand auger along north-facing hillslopes.

METHODS

This work builds upon an initial study of West et al. (2013), which presented data for two hillslopes within the SSHO watershed. Our expanded data set includes 44 new meteoric ¹⁰Be measurements from 4 additional hillslopes (2 north-facing and 2 south-facing); collectively, the 6 hillslopes span a range of average gradients from ~10-25° (SSHO range 15-20°; Fig. 1). Regolith samples were collected with a 5-cm-diameter hand auger until refusal in a 5 × 5 grid on planar hillslopes in each watershed (Fig. 1A). Sample locations were spaced ~5 m across slope and ~20 m downslope. Samples at each site were amalgamated by depth. We further mixed samples to the east and west of the central transect, so that three samples were analyzed for ¹⁰Be from ridge-top, mid-slope, and toe slope positions (Fig. DR1 in the GSA Data Repository¹). At the upper and lower slope positions, all five depth-amalgamated samples were mixed to one representative sample. Previous work showed that measured meteoric ¹⁰Be inventories are not affected by amalgamation (e.g., Jungers et al., 2009; West et al., 2013); therefore, we follow this approach here. Using these meteoric ¹⁰Be measurements, we evaluate transport rate laws and coefficients using gradients determined from a high-resolution digital elevation model.

RESULTS

Our results reveal that regolith thickness at the SSHO varies systematically with hillslope aspect (Figs. 1E and 1F). Along low-gradient, south-facing hillslopes, augerable regolith is relatively uniform (30–40 cm), with thicker (~80 cm) regolith present only at the toe of the slope. In contrast, augerable regolith is thicker (40–60 cm) along north-facing slopes and exhibits considerable variability in both the downslope and cross-slope directions (Fig. 1F).

Observations from hand excavations and soil pits within the SSHO watershed suggest that this variability reflects the presence of a buried 1–1.5-m-thick layer of angular colluvium on the north-facing hillside that mantles fractured bedrock (West et al., 2013). Within soil pits, we observe a distinct stratigraphy on the north-facing hillslope; massive, poorly structured regolith overlies a clast-supported framework of shale fragments as large as 5–10 cm in diameter (Fig. DR2). In contrast, the augerable, poorly structured regolith along south-facing hillslopes directly overlies weathered bedrock, and no coarse underlying colluvial material is present (Fig. DR2).

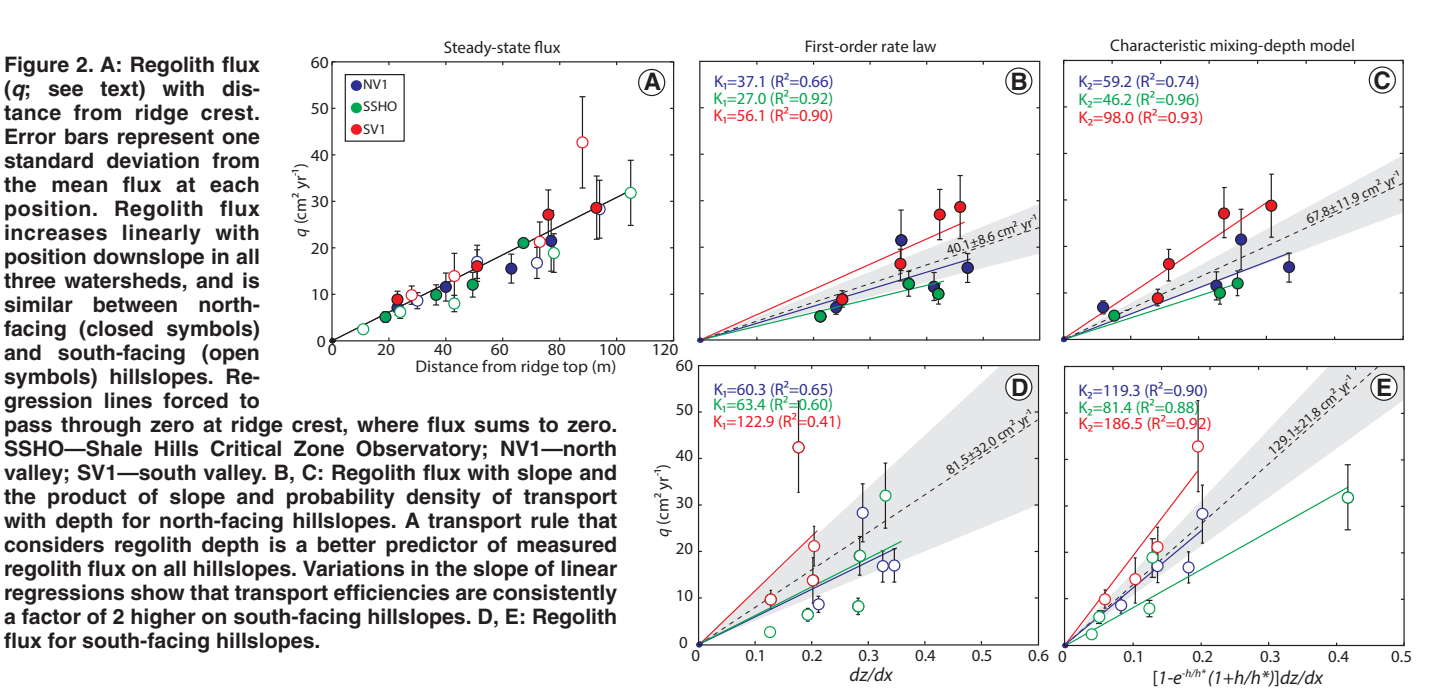
Meteoric 10Be concentrations in regolith are similar across all hillslopes and do not vary systematically with hillslope position, amalgamation technique, or aspect (Table DR1). Combining meteoric 10Be concentrations with depth-averaged regolith densities and an assumed meteoric 10Be delivery rate of 1.8×10^6 atoms cm⁻² yr⁻¹ (Graly et al., 2011), we estimate regolith flux (Equation 3). Our results suggest that regolith flux increases linearly with distance from ridge crests, and does not appear to vary with hillslope aspect (Fig. 2A). Rather, the similarity of flux patterns along sample transects appears to be consistent with spatially uniform lowering of the landscape at rates of \sim 20–30 m/m.y. over the past 10–15 k.y. (West et al., 2013). This similarity between regolith flux along north-facing and south-facing hillslopes suggests that ¹⁰Be is retained in the upper regolith and is not lost to deep colluvium.

To evaluate the applicability of geomorphic transport laws used to describe creeping regolith (Equations 1 and 2), we plot measured regolith flux against topographic gradient and mean regolith depth (Fig. 2). Along north-facing hillslopes, downslope regolith flux correlates with local topographic gradient (Fig. 2B), consistent with a slope-dependent transport rule (Equation 1). This correlation is poor along southfacing slopes (Fig. 2D), suggesting that such a rate law does not completely describe regolith creep. The correlation between regolith flux and a characteristic mixing depth model (Equation 2) is significantly stronger along both north-facing and south-facing slopes (Figs. 2C and 2E). Thus, our data imply that regolith flux depends on both regolith thickness and local gradient at this field site.

Our data suggest that transport efficiency $(K_1 \text{ or } K_2)$ is approximately two times greater along south-facing (equatorial-facing) slopes than along north-facing (polar-facing) slopes at the SSHO (Figs. 2B–2E). Assuming a characteristic mixing depth of 100 cm, consistent with the depth of root and frost penetration (Gaines

¹GSA Data Repository item 2014180, sampling and analytical methods with Figures DR1 and DR2, Table DR1 (meteoric ¹⁰Be concentrations), and Table DR2 (measured flux, hillslope gradient, and regolith depth), is available online at www.geosociety.org/pubs/ft2014.htm, or on request from editing@geosociety.org or Documents Secretary, GSA, P.O. Box 9140, Boulder, CO 80301, USA.

Figure 2. A: Regolith flux (q; see text) with distance from ridge crest. Error bars represent one standard deviation from the mean flux at each position. Regolith flux increases linearly with position downslope in all three watersheds, and is similar between northfacing (closed symbols) and south-facing (open symbols) hillslopes. Regression lines forced to



et al., 2013; nsidc.org/cryosphere/frozenground /whereis_fg.html), K, ranges from ~46-98 cm² yr⁻¹ on north-facing slopes (Fig. 2C), and 81 to 187 cm² yr⁻¹ on south-facing slopes (Fig. 2E). This difference is also apparent in the linear transport model; K_1 is 27–56 cm² yr⁻¹ on north-facing slopes, but 60-123 cm² yr⁻¹ on south-facing slopes (Figs. 2B and 2D). The difference in transport efficiency between hillslopes of opposing aspect is greater than variability in transport efficiency among hillslopes of similar aspect (Figs. 2B-2E). That the apparent asymmetry in transport efficiency does not depend on the form of the transport rule suggests the difference in efficiency between polarand equatorial-facing slopes is a robust result of our study.

DISCUSSION

Several lines of evidence suggest that the deep colluvial material along the north-facing slope of the SSHO does not currently participate in downslope creep or in the transport of meteoric ¹⁰Be. First, the rooting depth of large woody vegetation (Gaines et al., 2013) and the scale of pit-and-mound topography associated with tree-throw events appear to be ~1 m, near the top of the buried colluvium. Similarly, average freezing depths reach ~1 m in central Pennsylvania (nsidc.org/sites/nsidc.org/files/images //NA_permafrost.jpg), suggesting that freezethaw does not currently activate motion in the buried colluvium. In addition, the colluvial mantle retains a crude clast alignment reminiscent of structure in periglacial deposits (e.g., grèzes litées). Meteoric 10Be data from southfacing hillslopes, where the depth to refusal coincides directly with the boundary between disaggregated regolith and mechanically intact

(but fractured) rock, yields fluxes identical to those along north-facing hillsides, suggesting that these data capture most, if not all, of the mobile regolith transport.

The observation that regolith flux is equivalent on north-facing and south-facing slopes despite systematic differences in regolith depth and topographic gradient on opposing hillslopes provides quantitative evidence that microclimate variations associated with hillslope aspect influence the efficiency of regolith transport on soil-mantled hillsides. Although the total regolith flux from north-facing and south-facing hillslopes in our studied watersheds is equivalent within uncertainty (Fig. 2A), the differences in gradient and regolith depth along these hillslopes require more efficient regolith transport on south-facing hillslopes.

Our tests of transport rules at the SSHO suggests that considering the probability distribution of disturbance with regolith depth (e.g., Anderson, 2002; Anderson et al., 2013) provides a better characterization of regolith transport and erosion on hillslopes than a first-order rate law that depends solely on gradient. Our study thus bolsters a growing body of evidence in support of rules that incorporate regolith depth and/ or velocity gradients into landscape evolution models (e.g., Heimsath et al., 2005; Pelletier et al., 2011).

Tree species, tree density, and rooting depths are similar across the watershed (Gaines et al., 2013), suggesting no difference in bioturbation on north-facing and south-facing slopes. However, heave during freeze-thaw cycles may be controlled by aspect at the SSHO. Variations in stable isotope ratios in modern soil waters at the SSHO suggest enhanced snow melt and infiltration on south-facing hillslopes (Thomas et al.,

2013), as regolith on north-facing hillslopes remains frozen and shielded under snow pack for a greater fraction of the winter. Thus, these proxy data suggest the possibility that greater insolation on the south-facing hillslopes is associated with more frequent freeze-thaw and wettingdrying events. Because these processes are associated with slope-normal volumetric expansion and gravitational collapse of regolith that drive downslope creep (e.g., Anderson et al., 2013), we suggest that they provide a ready explanation for both the depth dependence of regolith transport and the variability in transport efficiency.

If we further consider that transport largely occurs during frost heave, we can relate transport to the contribution of freeze-thaw events. In this case, the transport efficiency of frost heave reflects the frequency and magnitude of freezethaw events, and K_2 is then transformed to

$$K_2 = \frac{1}{2} f \beta h^{*2} , \qquad (4)$$

where f is the frequency of freezing events (yr⁻¹), β is the strain associated with regolith expansion during freezing, and h^* is the maximum frost penetration depth (Anderson, 2002). Assuming that frost penetration depth and freezing strain do not change with aspect, freeze-thaw events must be twice as frequent on south-facing hillslopes as on north-facing hillslopes at the SSHO in order to account for the differences in transport efficiency. Therefore, the transport efficiencies observed at the SSHO suggest freeze-thaw frequencies of 0.1-0.2 yr⁻¹ for north-facing slopes and 0.2–0.4 yr⁻¹ for south-facing slopes. These values are consistent with modeled return periods of frost penetration to 100 cm in bare soil (no snow) for central Pennsylvania (DeGaetano et al., 1996).

The asymmetric topography in our study area suggests that the difference in transport efficiency has been sustained over geologic time. The combination of the location of the SSHO in the mid-latitudes, where annual fluctuations in temperature allow freeze-thaw processes to be relatively efficient, and the slow erosion and lowering of the Appalachian landscapes (Portenga et al., 2013) appears to have allowed microclimatic differences to be expressed in topography (e.g., Poulos et al., 2012). The proximity to the terminus of the Laurentide ice sheet would have enhanced frost-heave mediated transport during Pleistocene climate variations, potentially setting the stage for the modern observed aspect-related topographic asymmetry. Our data imply that topographic asymmetry observed at the SSHO, and perhaps elsewhere in the midlatitudes, represents an equilibrium solution to aspect-related microclimate differences even under conditions of uniform lowering and erosion over geologic time.

ACKNOWLEDGMENTS

We thank A. Neely and C. Regalla for field assistance, B. DeJong for ¹⁰Be extraction, and R. Anderson, A. Heimsath, and two anonymous reviewers. This work was supported by the National Science Foundation Critical Zone Observatories program (grants EAR-07-25019 and EAR-12-39285). West acknowledges support from a NASA Earth and Space Science Fellowship (NNX11AL72H).

REFERENCES CITED

- Anderson, R.S., 2002, Modeling of tor-dotted crests, bedrock edges and parabolic profiles of the high alpine surfaces of the Wind River Range, Wyoming: Geomorphology, v. 46, p. 35–58, doi:10.1016/S0169-555X(02)00053-3.
- Anderson, R.S., Anderson, S.P., and Tucker, G.E., 2013, Rock damage and regolith transport by frost: An example of climate modulation of the geomorphology of the critical zone: Earth Surface Processes and Landforms, v. 38, p. 299– 316, doi:10.1002/esp.3330.
- Burnett, B.N., Meyer, G.A., and McFadden, L.D., 2008, Aspect-related microclimatic influences on slope forms and processes, northeastern Arizona: Journal of Geophysical Research, v. 113, F03002, doi:10.1029/2007JF000789.
- Clark, G.M., and Ciolkosz, E.J., 1988, Periglacial geomorphology of the Appalachian highlands and interior highlands south of the glacial border—A review: Geomorphology, v. 1, p. 191–220, doi:10.1016/0169-555X(88)90014-1.
- Culling, W.E.H., 1963, Soil creep and the development of hillside slopes: Journal of Geology, v. 71, p. 127–161, doi:10.1086/626891.
- DeGaetano, A.T., Wilks, D.S., and McKay, M., 1996, Atlas of soil freezing depth extremes for the northeastern United States: Ithaca, New York, Cornell University, Northeastern Regional Climate Center Research Series Publication RR 96–1, 32 p.

- Gaines, K.P., Eissenstat, D., and Lin, H., 2013, Patterns in tree water extraction depth at the Susquehanna Shale Hills Critical Zone Observatory in central Pennsylvania: Ecological Society of America Annual Meeting, 4–9 August 2013, Minneapolis, Minnesota, abs. COS 60-1.
- Gilbert, G.K., 1904, Systematic asymmetry of crest lines in the High Sierra of California: Journal of Geology, v. 12, p. 579–588, doi:10.1086/621182.
- Graly, J.A., Reusser, L.J., and Bierman, P.R., 2011, Short and long-term delivery rates of meteoric ¹⁰Be to terrestrial soils: Earth and Planetary Science Letters, v. 302, p. 329–336, doi:10.1016/j .epsl.2010.12.020.
- Hack, J.T., and Goodlett, J.C., 1960, Geomorphology and forest ecology of a mountain region in the central Appalachians: U.S. Geological Survey Professional Paper 343, 66 p.
- Heimsath, A.M., Furbish, D.J., and Dietrich, W.E., 2005, The illusion of diffusion: Field evidence for depth dependent sediment transport: Geology, v. 33, p. 949–952, doi:10.1130/G21868.1.
- Istanbulluoglu, E., Yetemen, O., Vivoni, E.R., Gutiérrez-Jurado, H.A., and Bras, R.L., 2008, Ecogeomorphic implications of hillslope aspect: Inferences from analysis of landscape morphology in central New Mexico: Geophysical Research Letters, v. 35, L14403, doi:10.1029/2008GL034477.
- Jungers, M.C., Bierman, P.R., Matmon, A., Nichols, K., Larsen, J., and Finkel, R., 2009, Tracing hillslope sediment production and transport with in situ and meteoric ¹⁰Be: Journal of Geophysical Research, v. 114, no. F4, doi:10.1029 /2008JF001086.
- Kirkby, M.J., 1971, Hillslope process-response models based on the continuity equation, in Brunsden, D., ed., Slopes: Form and process: Institute of British Geographers Special Publication 3, p. 15–30.
- Ma, L., Chabaux, F., West, N., Kirby, E., Jin, L., and Brantley, S., 2013, Regolith production and transport in the Susquehanna Shale Hills Critical Zone Observatory, Part 1: Insights from U-series isotopes: Journal of Geophysical Research, v. 118, p. 722–740, doi:10.1002/jgrf.20037.
- McKean, J.A., Dietrich, W.E., Finkel, R.C., Southon, J.R., and Caffee, M.W., 1993, Quantification of soil production and downslope creep rates from cosmogenic ¹⁰Be accumulations on a hill-slope profile: Geology, v. 21, p. 343–346, doi: 10.1130/0091-7613(1993)021<0343:QOSPAD >2.3.CO;2.
- Melton, M.A., 1960, Intravalley variation in slope angles related to microclimate and erosional environment: Geological Society of America Bulletin, v. 71, p. 133–144, doi:10.1130/0016-7606(1960)71[133:IVISAR]2.0.CO;2.
- Monaghan, M.C., McKean, J., Dietrich, W., and Klein, J., 1992, ¹⁰Be chronometry of bedrock-to-soil conversion rates: Earth and Planetary Science Letters, v. 111, p. 483–492, doi:10.1016/0012-821X(92)90198-5.
- Naylor, S., and Gabet, E.J., 2007, Valley asymmetry and glacial versus nonglacial erosion in the Bitterroot Range, Montana, USA: Geology, v. 35, p. 375–378, doi:10.1130/G23283A.1.
- Pelletier, J.D., McGuire, L.A., Ash, J.L., Engelder, T.M., Hill, L.E., Leroy, K.W., Orem, C.A.,

- Rosenthal, W.S., Trees, M.A., Rasmussen, C., and Chorover, J., 2011, Calibration and testing of upland hillslope evolution models in a dated landscape: Banco Bonito, New Mexico: Journal of Geophysical Research, v. 116, no. F4, doi:10.1029/2011JF001976.
- Perron, J.T., Kirchner, J.W., and Dietrich, W.E., 2009, Formation of evenly spaced ridges and valleys: Nature, v. 460, p. 502–505, doi:10.1038 /nature08174.
- Pierce, K.L., and Colman, S.M., 1986, Effect of height and orientation (microclimate) on geomorphic degradation rates and processes, late glacial terrace scarps in central Idaho: Geological Society of America Bulletin, v. 97, p. 869–885, doi: 10.1130/0016-7606(1986)97<869:EOHAOM> 2.0.CO;2.
- Portenga, E.W., Bierman, P.R., Rizzo, D.M., and Rood, D.H., 2013, Low rates of bedrock outcrop erosion in the central Appalachian Mountains inferred from in situ ¹⁰Be: Geological Society of America Bulletin, v. 125, p. 201–215, doi:10.1130/B30559.1.
- Poulos, M.J., Pierce, J.L., Flores, A.N., and Benner, S.G., 2012, Hillslope asymmetry maps reveal widespread, multi-scale organization: Geophysical Research Letters, v. 39, L06406, doi:10.1029 /2012GL051283.
- Roering, J.J., 2008, How well can hillslope evolution models "explain" topography? Simulating soil transport and production with high-resolution topographic data: Geological Society of America Bulletin, v. 120, p. 1248–1262, doi:10.1130 /B26283.1.
- Thomas, E.M., Lin, H., Duffy, C.J., Sullivan, P.L., Holmes, G.H., Brantley, S.L., and Jin, L., 2013, Spatiotemporal patterns of water stable isotope compositions at the Shale Hills Critical Zone Observatory: Linkages to subsurface hydrologic processes: Vadose Zone Journal, v. 12, no. 4, doi:10.2136/vzj2013.01.0029.
- West, N., Kirby, E., Bierman, P., Slingerland, R., Ma, L., Rood, D., and Brantley, S., 2013, Regolith production and transport at the Susquehanna Shale Hills Critical Zone Observatory, Part 2: Insights from meteoric ¹⁰Be: Journal of Geophysical Research, v. 118, doi:10.1002/jgrf.20121.
- Willenbring, J.K., and von Blanckenburg, F., 2010, Meteoric cosmogenic Beryllium-10 adsorbed to river sediment and soil: Applications for Earthsurface dynamics: Earth-Science Reviews, v. 98, p. 105–122, doi:10.1016/j.earscirev.2009 .10.008.
- Yoo, K., Amundson, R., Heimsath, A.J., Dietrich, W.E., and Brimhall, G.H., 2007, Integration of geochemical mass balance with sediment transport to calculate rates of soil chemical weathering and transport on hillslopes: Journal of Geophysical Research, v. 112, F02013, doi:10.1029 /2005JF000402.

Manuscript received 5 December 2013 Revised manuscript received 15 March 2014 Manuscript accepted 18 March 2014

Printed in USA